Biochemistry and Biophysics Reports 36 (2023) 101573

Contents lists available at ScienceDirect

Biochemistry and Biophysics Reports

journal homepage: www.elsevier.com/locate/bbrep

Control of A/D type CpG-ODN aggregates to a suitable size for induction of strong immunostimulant activity

Miyu Matsuda, Shinichi Mochizuki *

Department of Chemistry and Biochemistry, The University of Kitakyushu, 1-1 Hibikino, Wakamatsu-ku, Kitakyushu, Fukuoka, 808-0135, Japan

ARTICLE INFO

Keywords:
CpG-ODN
Adjuvant
Toll-like receptor 9
G-quadruplex

ABSTRACT

Among several types of CpG-ODNs, A/D-type CpG-ODNs have potent adjuvant activity to induce Th-1 immune responses, but exhibit a propensity to aggregate. For the clinical application of A/D-type CpG-ODNs, it is necessary to control such aggregation and obtain a comprehensive understanding of the relationship between their structure and the immune responses. This study revealed that a representative A/D-type CpG ODN, D35, adopted a single-stranded structure in water, while it assembled into aggregates in response to Na^+ ions. From polyacrylamide gel electrophoresis and circular dichroism analyses, D35 adopted a homodimeric form (duplex) via palindromic sequences in low-Na^+-concentration conditions (10–50 mM NaCl). After replacement of the solution with PBS, quadruplexes began to form in a manner coordinated by Na^+, resulting in large aggregates. The duplexes and small aggregates prepared in 50 mM NaCl showed not only high cellular uptake but also high affinity to Toll-like receptor 9 (TLR9) proteins, leading to the production of a large amount of interferon-α for peripheral blood mononuclear cells. The much larger aggregates prepared in 100 mM NaCl were incorporated into cells at a high level, but showed a low ability to induce cytokine production. This suggests that the large aggregates have difficulty inducing TLR9 dimerization, resulting in loss of the stimulation of the cells. We thus succeeded in inducing adequate innate immunity *in vitro* by controlling and adjusting the formation of D35 aggregates. Therefore, the findings in this study for D35 ODNs could be a vital research foundation for *in vivo* applications.

1. Introduction

Unmethylated cytosine-phosphate-guanine dinucleotides, known as CpG motifs, are recognized by one of the pattern recognition receptors, Toll-like receptor 9 (TLR9), which has the ability to detect certain distinctive sequences in pathogens but not in self-genomes [1]. The interaction between oligonucleotides (ODNs) containing CpG motifs and TLR9 induces strong Th-1 immune responses rather than Th-2 responses [2,3]. Therefore, the potent adjuvant activity of CpG-ODNs has been studied based on their use as a component of vaccines.

Considering the chemical backbone and sequence characteristics, CpG ODNs are classified into four categories: A/D-, B/K-, C-, and P-type ODNs [4–6]. Among them, A/D-type CpG-ODNs have a phosphodiester palindromic domain in the central region, which contains one or more CpG motifs in the palindrome [7,8]. Furthermore, A/D-type CpG-ODNs have poly(G) sequences with a phosphorothioate backbone at the 5′ and 3′ ends. This class of CpG-ODNs can induce high levels of interferon-α (IFN-α) production in plasmacytoid dendritic cells (pDCs), while they have a low ability to stimulate TLR9-dependent NF-κB signaling [9,10]. IFN-α activates the CD8-positive cytotoxic T lymphocyte response. The activated pDCs also secrete IL-12, which promotes the differentiation of Th-0 into Th-1 [11]. Compared with A/D-type CpG-ODNs, B/K-type CpG-ODNs can stimulate many genes associated with resistance to bacterial infection, such as IL-1β and IL-6 [11]. C-type CpG-ODNs combine the characteristics of the A/D- and B/K-type CpG-ODNs, inducing IL-6 and IFN-α. However, its ability to induce IFN-α is lower than that of type A CpG-ODNs [12]. Although the feature of B/K- and C-type CpG-ODNs is to have phosphorothioate structures in their backbones, some reports showed the toxicity derived from the unnatural phosphorothioate backbones [13,14]. Taking these findings together, A/D-type CpG-ODNs are expected to be utilized as an adjuvant with high safety to induce strong protective immune responses.

Such a strong IFN-α induction by A/D-type ODNs is associated with the higher-order structure of the ODNs [7,15,16]. The poly(G) sequences at the 5′ and 3′ ends readily induce the formation of ODN multimerization in a salt solution, resulting in large aggregates. The

* Corresponding author.
E-mail address: mochizuki@kitakyu-u.ac.jp (S. Mochizuki).

https://doi.org/10.1016/j.bbrep.2023.101573
Received 4 July 2023; Received in revised form 29 October 2023; Accepted 31 October 2023

formation of aggregates is essential for A/D-type ODNs to induce high levels of IFN-α production. However, this presents a huge obstacle to their clinical application [17]. The uncontrolled aggregation and precipitation by ODN multimerization can stimulate other signaling pathways and induce unexpected side effects.

The formation and stability of the structures induced by ODNs with guanine-rich sequences are attributed to Hoogsteen hydrogen bonding among four guanines, which is specifically coordinated by alkali metal ions such as sodium and potassium ions [18,19]. These structures (G-quadruplexes) are drawing increasing attention and are used as building blocks of DNA nanotechnologies such as DNA nanomachines and nanomedicines [20,21]. Because appropriate and accurate DNA assemblies are critical for G-quadruplex-based nanotechnologies, the structural features and kinetics when changing the types of alkali metal ions and the salt concentration have been studied for various ODNs with guanine-rich sequences [19,22]. In this study, we demonstrated the preparation of various assemblies consisting of D35 ODN [17], a representative A/D-type CpG ODN, by changing the sodium ion concentration and evaluated the affinity to the TLR9 protein and the adjuvant activity for human peripheral blood mononuclear cells (PBMCs).

2. Materials and methods

2.1. Materials

D35 (5′-GˆGTGCATCGATGCAGGGGˆGˆG-3′: ˆ indicates a phosphorothioate backbone) was synthesized by Gene Design Co., Ltd. (Osaka, Japan). Dynabeads Protein G Immunoprecipitation Kit and recombinant mouse TLR9 Fc chimera (mTLR9Fc) were purchased from Thermo Fisher Scientific (Waltham, MA) and R&D Systems (Minneapolis, MN), respectively.

2.2. Preparation of D35 aggregation

The sample tubes containing D35 containing were added to a water bath maintained at 95 °C. After incubation for 5 min, the temperature setting was removed. The tubes were allowed to stand overnight and then slowly cooled to room temperature.

2.3. Polyacrylamide gel electrophoresis (PAGE)

For the preparation of PAGE, 50 μM D35 in water, 10 mM NaCl, 50 mM NaCl, and 100 mM NaCl solutions were annealed. After replacing each solution with 10 × phosphate-buffer saline (PBS), the samples were left to stand at room temperature for the indicated times. D35 (10 ng) was separated using a 12 % acrylamide gel for 1 h at 100 V. After the gel had been stained with SYBR Gold (Invitrogen, Carlsbad, CA), fluoresce imaging was performed using a PharosFX (Bio-Rad, Richmond, CA).

2.4. Circular dichroism (CD) spectroscopy

After D35 solutions (15 μM D35 in water, 10 mM NaCl, 50 mM NaCl, and 100 mM NaCl) had been replaced with PBS and left to stand for the indicated times, they were subjected to CD analysis. The CD in the wavelength region of 240–320 nm was measured on a Jasco J-802 spectropolarimeter (JASCO, Tokyo, Japan) at 25 °C using a 1 cm quartz cell with a water jacket.

2.5. In vitro uptake of D35 into cells

DC2.4 cells (mouse dendritic cell line) were purchased from Millipore Corporation (Temecula, CA) and cultured in RPMI-1640 medium (FUJIFILM Wako Pure Chemical Corporation, Osaka, Japan) containing 10 % FBS, 100 U/mL penicillin, 0.1 mg/mL streptomycin, and 0.5 % β-mercaptoethanol (FUJIFILM Wako Pure Chemical Corporation). DC2.4 cells were seeded at 3.0×10^5 cells/well in 12-well plates and supplemented with FITC-labeled D35 (Gene Design) at 1 μM. After incubation for 3 h, the cells were washed with PBS three times and the fluorescence intensity of the cells was observed using a flow cytometer (CytoFLEX; Beckman Coulter, Fullerton, CA).

2.6. Immunoprecipitation binding assay

Magnetic beads (25 μl) and 5 μg of mTLR9Fc (50 μl) were mixed and incubated for 20 min with rotation at a speed of 10 rpm at 25 °C [22]. After washing once with the binding and washing buffer, the Dynabeads-mTLR9Fc complex was resuspended in PBS. A total of 500 pmol D35 in water, 10 mM NaCl, 50 mM NaCl, or 100 mM NaCl was added to the Dynabeads-mTLR9Fc complex and incubated for 1 h with rotation at 25 °C. After washing three times with washing buffer and removing the unbound D35, 10 μl of elution buffer was added and incubated at 25 °C for 15 min to release D35 from the Dynabeads-mTLR9Fc complex. The supernatants were subjected to 12 % PAGE and visualized by SYBR Gold staining. At 3 h after the replacement of D35 with PBS when the sample had been left to stand at room temperature, the D35 bound to the Dynabeads-mTLR9Fc complex was assessed in the same way.

2.7. Cell viability assay

Human PBMC samples were obtained from iQ Biosciences (Berkeley, CA) and cultured in RPMI-1640 medium containing 10 % FBS, 100 U/mL penicillin, and 0.1 mg/mL streptomycin. After 24 h of treatment with D35 at 1 μM for human PMBCs, the medium was changed to a medium containing tetrazolium salt (WST-1; Dojindo, Kumamoto, Japan) and incubated for 6 h. Formazan is then produced by succinate-tetrazolium reductase in living cells. The absorbance at 450 nm was measured using a microplate reader (Multiskan FC; Thermo Fisher Scientific).

2.8. Cytokine production from PBMCs by stimulation with D35

PBMCs were seeded at 1.0×10^6 cells/well in 96-well plates and supplemented with D35 at 1 μM. After 24 h, the amount of IFN-α secreted into the supernatants was measured with an IFN-alpha Human ELISA Kit (Thermo Fisher Scientific).

2.9. Statistical analysis

All data are presented as mean ± SD. The statistical significance of differences between two groups was analyzed using two-tailed Student's *t*-test.

3. Results

3.1. Structures of D35 at different NaCl concentrations

In this study, we focused on the effect of sodium ions (Na^+) on the structures formed by D35 because the Na^+ concentration is much higher than that of potassium ions (K^+) in the extracellular environment. D35 in the solution with each different NaCl concentration was annealed and subjected to 12 % PAGE analysis (Fig. 1A). D35 prepared in water showed a single band, while D35 prepared in solution containing NaCl showed new bands at a higher molecular weight besides the band observed in water. The intensity of the bands observed at a higher molecular weight increased in a NaCl concentration-dependent manner. Furthermore, some D35 prepared in 100 mM NaCl formed aggregates that were too large to migrate in the gel. These results indicate that D35 responds sensitively to Na^+ and forms aggregates. In this study, the bands observed at a higher molecular weight than in the D35 control and the aggregates that could not migrate in the gel are hereinafter referred to as low-D35 aggregates (L-D35) and high-D35 aggregates (H-D35), respectively (Fig. 1A). Incidentally, the structure taken by D35

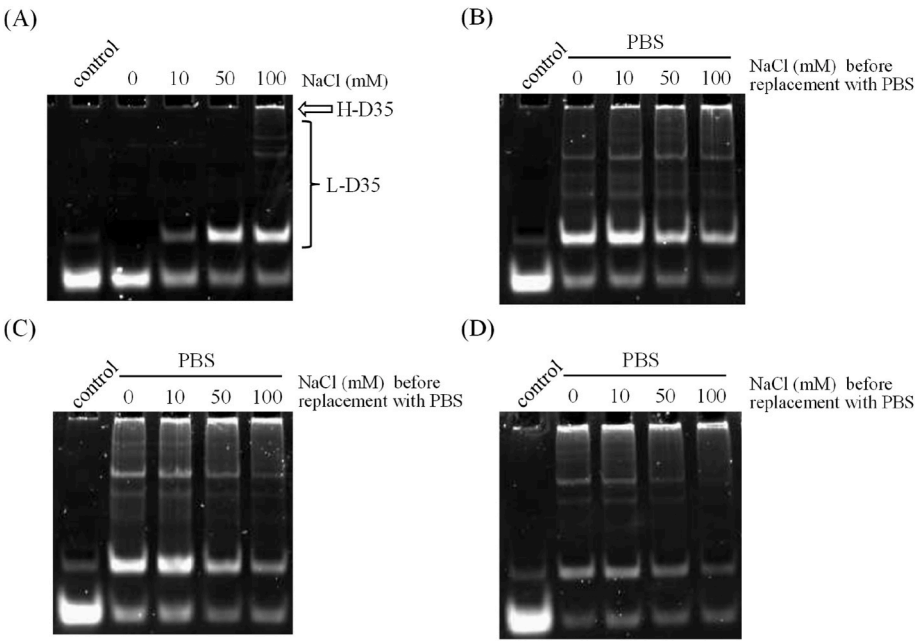

Fig. 1. PAGE migration patterns of D35. (A) 50 μM of D35 in the indicated NaCl solution was annealed and subjected to 12 % PAGE. The bands observed at a higher molecular weight than the D35 control and the bands that could not migrate in the gel were determined to be L-D35 and H-D35, respectively. After the replacement of each NaCl solution with PBS, each D35 solution was left to stand for 30 min (B), 3 h (C), or 24 h (D), and subjected to 12 % PAGE.

depended on the type of alkali metal ion. After annealing D35 in solutions containing lithium chloride (LiCl) or KCl, D35 showed a different migration pattern than D35 in solutions containing NaCl. In 100 mM NaCl, some D35 formed H-D35, while in 100 mM LiCl, D35 did not form H-D35 at all (Supplementary Fig. 1). Furthermore, in KCl solution, most D35 formed H-D35 even in 10 mM KCl concentration. These results indicate that the formation and the amount of L-D35 and H-D35 depends on the size of the alkali metal ion and the concentration.

To investigate the stability of the aggregates under physiological conditions, each solution was replaced with PBS, left to stand for the indicated times, and subjected to PAGE analysis. Although there was no aggregation in the conditions with no NaCl, L-D35 appeared after the sample was left to stand for 30 min in PBS (Fig. 1B). The amount of L-D35 decreased with increasing NaCl concentration of the initial conditions, while the amount of H-D35 increased. After 3 h of being left to stand in PBS, some H-D35 was observed even for D35 in water at 0 h (Fig. 1C). After 24 h, all samples showed almost the same findings on electrophoresis (Fig. 1D), indicating the attainment of equilibrium regardless of the initial conditions. These results indicate that D35 adopts a single-stranded structure in water, but forms an L-D35 aggregate in a manner dependent on the NaCl concentration. Under conditions with higher NaCl, PBS, D35 forms H-D35 aggregates in a time-dependent manner.

Fig. 2A–D shows the CD spectra in the range of 210–320 nm for D35 before and after the replacement with PBS. CD measurement is a powerful tool to determine the secondary structures and conformations adopted by nucleic acids [23]. D35 in water showed a negative peak at 240 nm and a positive peak at 265 nm, which is a typical CD spectrum of the B-form of ODNs [24]. Although the spectral shapes almost matched that in water, even in the conditions with NaCl, the peak around 290 nm increased in intensity with increasing NaCl concentration (Supplementary Fig. 2). This indicates that the conformation was slightly changed by the presence of NaCl. After the replacement with PBS, the positive peak at 265 nm increased in intensity with time regardless of the initial conditions. Although G-quadruplexes adopt many types of structures, all of them are based on guanine tetrads. The spectra of parallel quadruplexes predominantly feature a positive peak at 260 nm, while those of anti-parallel quadruplexes feature a negative peak at 260 nm and a positive peak at 290 nm [25,26]. Considering this, D35 in NaCl solution can form hybrid (mixture of parallel and anti-parallel) quadruplexes by chelating Na^+. At 24 h, all D35 showed the same CD spectra. The spectrum changes observed in CD measurements agreed with the migration patterns in PAGE.

3.2. Uptake of D35 into DC2.4 cells

Because TLR9 exists in endosomal compartments, cytokine production can depend on the amount of D35 uptake. FITC-labeled D35 prepared in the solution with different NaCl concentrations was added to the DC2.4 cell culture medium. After 3 h of incubation at 37 °C, the fluorescence intensity of the cells was evaluated. The amount of D35 uptake into the cells increased with increasing initial NaCl concentration in the preparation (Fig. 3A). The cells treated with D35 prepared in 50 mM and 100 mM NaCl showed especially high intensities. If the cellular uptake reached a plateau soon after the addition of D35, the amount of uptake is considered to be influenced by the size and structure of aggregates and is preferred not small size but large size D35 (L-D35 and H-D35). In the case of the gradual uptake during 3 h, we should think about the influence of D35 aggregation in response to NaCl (Fig. 1). Because the Na^+ and K^+ ion concentrations in RPMI-1640 are 140 mM and 5.4 mM, respectively, the structures in the medium can be predominantly controlled by adjusting the Na^+ concentration. From Fig. 1C, most D35 forms L-D35 and H-D35 aggregates regardless of the initial conditions, after being left to stand for 3 h in PBS. The D35 structures adopted can depend on not only Na^+ concentration and the time spent under those conditions but also the concentration of D35 itself. The concentration of D35 prepared as shown in Fig. 1 (PAGE analysis) is 50 μM, while the concentration in the cellular uptake is 1 μM. When the concentration of D35 is much lower, it can take a long time to form the same aggregates as observed in Fig. 1 (Fig. 3B). In fact, after being left to stand for 3 h in PBS at 1 μM, the amounts of L-D35 and H-D35 aggregates prepared in 0 and 10 mM NaCl were far less than those prepared at 50 μM. Taking these findings together, the cells took up D35 in the form of not a single-stranded structure but aggregates (L-D35 and H-D35). Notably, the larger the aggregates were, the more cells preferred them.

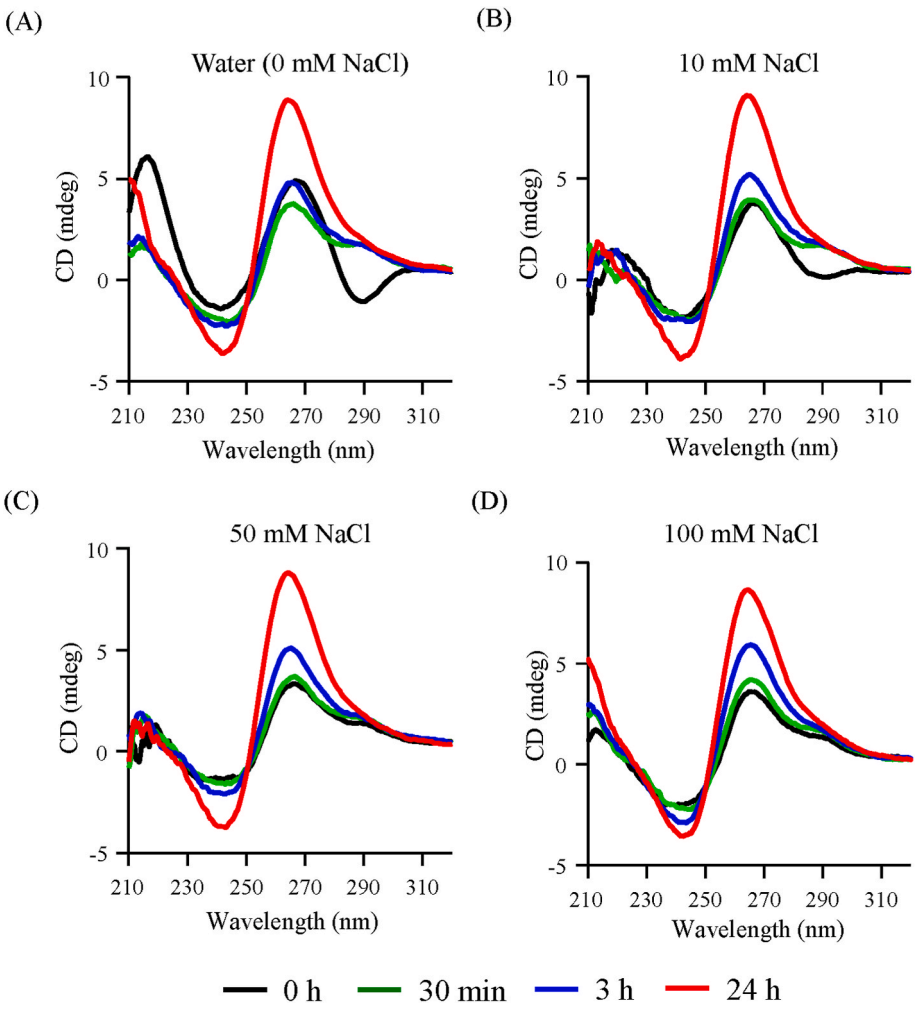

Fig. 2. CD spectra of the D35 solutions with NaCl concentrations of 0 (A), 10 (B), 50 (C), and 100 mM (D) after the replacement with PBS and being left to stand for the indicated times.

3.3. Interaction between D35 and mTLR9Fc

After internalization into cells, D35 binds to TLR9, resulting in the stimulation of DCs. To examine the relationship between the ability of D35 to bind to TLR9 and the structures, D35 bound to the mTLR9Fc protein was assessed by immunoprecipitation (Fig. 4A). Before the replacement with PBS, D35 prepared in 10 mM and 50 mM NaCl was bound to mTLR9Fc, while D35 prepared in water was not (Fig. 4B). Although D35 prepared in 100 mM NaCl was also bound to mTLR9Fc, the affinity was much lower than that of D35 prepared in 10 and 50 mM NaCl. At a high condition of NaCl concentration, because D35 is easy to aggregate and is difficult to take at the same structure, the ratio of L-D35 and H-D35 is considered to be different a little in every preparation in 100 mM NaCl. This causes the different affinity from D35 prepared in 50 mM NaCl although observed in the same structural pattern in Fig. 1A. We could not observe the bound D35 from the mixture of D35 prepared in 50 mM NaCl at the initial conditions and the magnetic beads without mTLR9Fc proteins (Supplementary Fig. 3). These results indicate that D35 adopting not a single-stranded structure but rather some aggregates specifically bound to mTLR9Fc proteins. After being left to stand for 3 h in PBS, D35 prepared in water, 10 mM and 50 mM NaCl bound to mTLR9Fc proteins, while D35 in 100 mM NaCl showed almost the same affinity as that before the replacement with PBS (Fig. 4C). Considering the state of D35 in each solution (Fig. 1), the affinity between D35 and mTLR9Fc proteins depends on the size of D35 aggregates. The aggregates with the size of L-D35 can strongly bind to mTLR9Fc proteins. The affinity decreased with aggregate sizes larger than L-D35, and H-D35 had a little binding affinity to mTLR9Fc proteins.

3.4. IFN-α production upon treatment with D35

IFN-α promotes adaptive immune responses and contributes to anti-tumor immunity by increasing the function of DCs, T cells, and NK cells [27]. At first, the cell viability was examined after treatment with D35. The treatment with D35 prepared in the indicated NaCl solution showed no cytotoxicity for PMBCs (Supplementary Fig. 4), indicating that we can discuss the amount of IFN-α production without considering the cytotoxicity by D35. The addition of D35 prepared in 50 mM and 100 mM NaCl to PBMCs induced the high production of IFN-α (Fig. 5). Although D35 prepared in water or 10 mM NaCl also stimulated PBMCs, the amount of IFN-α production was lower than that when prepared in 50 mM NaCl. This is considered to be attributable to the poor uptake into the cells (Fig. 3), regardless of having the ability to bind to TLR9 (Fig. 4C). Some PBMCs were not sufficiently stimulated by D35 prepared in 100 mM NaCl (Donor C in Fig. 5). Although D35 prepared in 100 mM NaCl is readily incorporated into the cells (Fig. 3), it has low affinity to TLR9 (Fig. 4C). Because the cells that induced IFN-α production can incorporate D35 before growing to the size that is too large to bind to TLR9, they could be activated by the D35 (Donors A and B). These results suggest that D35 prepared in 50 mM NaCl was suitable for incorporation into the cells and binding to TLR9 although the sensitivity is affected by individual variability. The aggregation of D35, such as

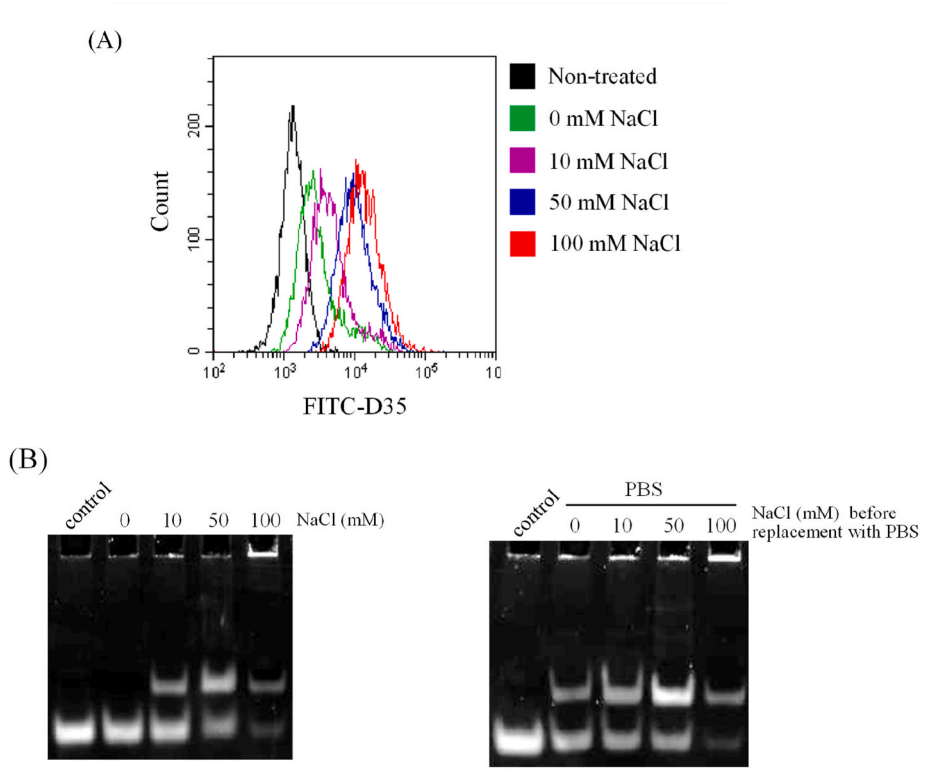

Fig. 3. Cellular uptake of D35. (A) D35 prepared in the indicated NaCl solution was added to DC2.4 cells at a concentration of 1 μM. After incubation for 3 h, the cells were subjected to flow cytometry. (B) PAGE migration patterns of D35 prepared at 1 μM. Before (left) and after (right) being left to stand for 3 h in PBS, each D35 solution was subjected to 12 % PAGE.

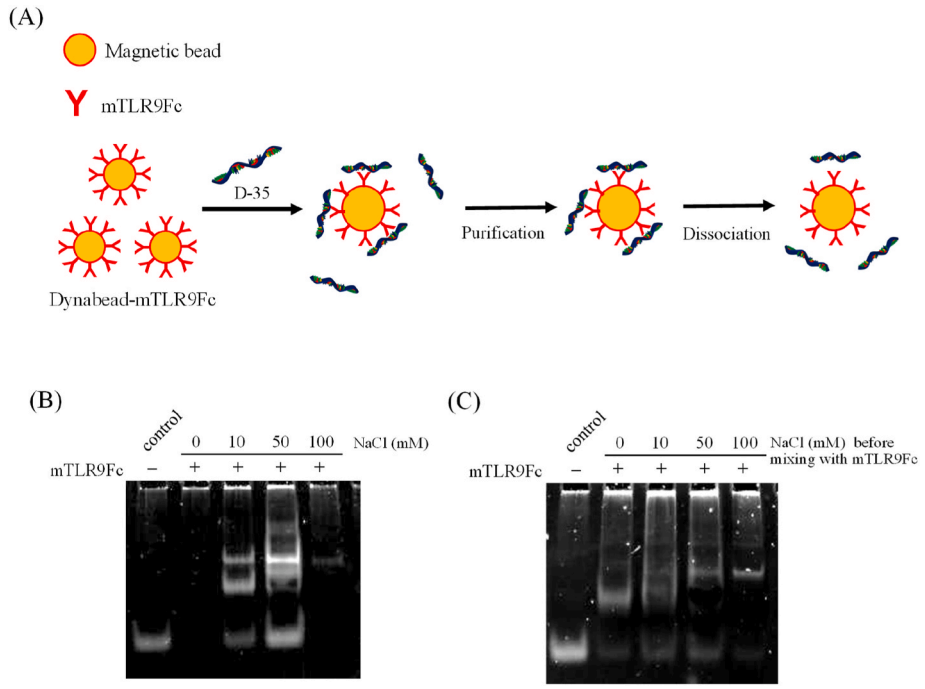

Fig. 4. Immunoprecipitation of D35 bound to mTLR9Fc proteins. (A) Schematic illustration of the immunoprecipitation assay. (B) D35 prepared in the indicated NaCl solution was incubated with the Dynabeads-mTLR9Fc complex. After incubation for 1 h, the D35 bound to mTLR9Fc proteins was subjected to 12 % PAGE. (C) After the replacement of D35 solution from the indicated NaCl solution with PBS and being left to stand for 3 h, D35 was incubated with the Dynabeads-mTLR9Fc complex.

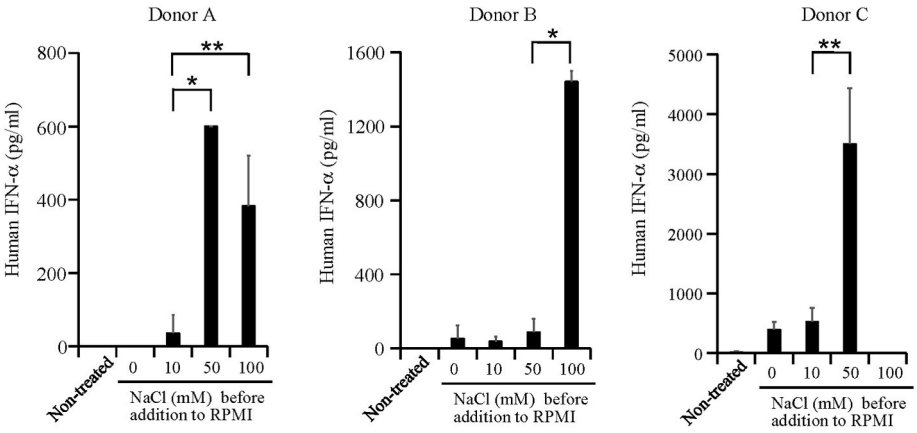

Fig. 5. Adjuvant activity by D35. Human PBMCs from three different donors were stimulated with the D35 prepared in the indicated NaCl solution for 24 h. IFN-α secreted in the supernatants was determined with an IFN alpha Human ELISA Kit. Non-treated means cells not stimulated with D35. Results are presented as the mean ± S.D. ($n = 3$). *$p < 0.01$, **$p < 0.05$.

L-D35, is essential not only for recognition by the cells but also for stimulating TLR9. In various situations including *in vivo* experiments, if we control the aggregation by preparing D35 in an appropriate NaCl solution, as shown in this study, it could be possible to induce adequate innate immunity.

4. Discussion

A/D-type CpG-ODNs such as D35 have the features of both potent adjuvant activity to induce Th-1 immune responses and difficulty for use in treatment given their propensity to aggregate. To apply A/D-type CpG-ODNs clinically, it is necessary to obtain a comprehensive understanding of their structural changes in response to the environment and the relationship between their structure and the machinery of immune induction. The present study demonstrates the influence of sodium ions on the structures adopted by D35 aggregates, and their subsequent cellular uptake and interaction with TLR9 proteins.

D35 adopts a single-stranded structure in water, but exhibits aggregation in response to sodium ions, resulting in large aggregates (Fig. 1). This aggregation involves several steps, which depend on the sodium ion concentration. D35 forms aggregates in a way that differs from other guanine-rich ODN sequences, establishing G-quadruplexes structures observed in such as telomeres and some aptamers because D35 contains guanine residues only at the 5′ and 3′ ends. Hertmann et al. advocated the following steps for the growth of aggregates by A/D-type CpG ODNs [7]. (1) Two A/D type CpG ODN monomers form a duplex via Watson-Crick base pairing of their palindromic sequences. (2) Two duplexes form a quadruplex via guanine-rich regions. (3) Another duplex is linked via a G-tetrad, resulting in an extension of the polymer. In this study, in water, hybridization between the palindromic sequences of two D35 ODNs was not induced because of the strong electrostatic repulsions between the phosphate backbones. The mitigated electrostatic repulsions in 10 mM and 50 mM NaCl solutions made it possible for hybridization to occur, resulting in the formation of a D35 duplex. Considering the size of the D35 duplex, it could account for the main band among L-D35 observed in Fig. 1A. CD spectra of D35 in 10 mM and 50 mM NaCl have a positive peak at 290 nm, while that in water does not. This suggests that double-stranded DNA was formed. The ratio of the intensities of the peaks of D35 between 10 mM and 50 mM NaCl (Fig. 2B and C) also corresponds to the abundance ratio of the duplex observed in PAGE (Fig. 1B and C). Furthermore, when D35 was subjected to gel permeation chromatography using 50 mM NaCl solution as a mobile phase, a single peak was observed. From multi-angle light scattering analysis, the weight-averaged molecular weight (M_w) of D35 in 50 mM NaCl was calculated to be $M_w = 1.5 \times 10^4$ (data not shown), which is close to the theoretical value of 1.3×10^4. These results indicate that the main band among L-D35 (Fig. 1A) is the D35 duplex. Under conditions of approximately 150 mM NaCl, Na^+ gradually began to be chelated between two duplexes and subsequently the quadruplexes formed. However, the high concentration of Na^+ accelerated rapid polymerization among the quadruplexes, resulting in the formation of H-D35. Therefore, we could only observe weak bands derived from the small quadruplexes, which appeared between the D35 duplex and H-D35 in PAGE (Fig. 1B–D). The formation of quadruplexes also indicates the formation of Hoogsteen base pairing of the G-quadruplex and suggests the dissociation of the duplex of CpG motifs. This is possible because Watson-Crick base pairing of the original duplex is weakened by the neighboring new Hoogsteen base pairing [28]. Although the dissociation of the duplex also means the disappearance of the peak at 290 nm in the CD spectrum, the peak was retained in the conditions with NaCl concentration of around 150 mM (Fig. 2). This indicates that the quadruplexes adopt a hybrid structure containing both parallel and anti-parallel orientations, showing distinctive positive peaks at 260 nm and 290 nm.

Recent research has revealed that some cells expressing TLR9 also have receptors for DNAs including CpG-ODNs on their surface, such as receptor for advanced glycation end products (RAGE), C-type mannose receptor 1 (MRC1), and macrophage scavenger receptor 1 (MSR1) [29–31]. We previously demonstrated that K/B-type ODN with a length of more than 30mer and multiple CpG motifs can be recognized by MRC1-expressing APCs [32]. This indicates that multiple interactions between the CpG motif and the receptor promote cellular uptake. In this study, there is a possibility of the promotion of interactions between the L-D35 or H-D35 aggregates and multiple receptors on the cells. As a result, the cellular uptake of L-D35 and H-D35 was enhanced, compared with that for single-stranded D35 (Fig. 3). Although certain receptors would recognize the CpG motif, double-stranded D35, or the quadruplex, the issue of which parts of the aggregates are essential for cellular uptake should be investigated further in future work.

TLR9 is known to require dimerization through binding to CpG-ODN for activation of the immune system [33,34]. Because the formation of a TLR9 dimer requires that CpG-ODNs are positioned close to each other, after the first binding to TLR9, the D35 aggregates largely increase the probability of accessing the following TLR9 compared with a single-stranded D35. Considering this, the interaction between multiple D35 and TLR9 can be stronger than that between single-stranded D35 and TLR9. In the immunoprecipitation assay, the binding between L-D35 and mTLR9Fc was observed, while the binding between single-stranded D35 and mTLR9Fc was not (Fig. 4B). Interestingly, H-D35 decreased the binding affinity to mTLR9Fc. This suggests that much larger aggregates with low flexibility have difficulty binding to another TLR9 protein after the first binding. In addition, the large

aggregates adopted by D35 are easy to precipitate [17], resulting in loss of the chance to bind to mTLR9Fc proteins. In fact, the treatment with H-D35 did not always induce IFN-α production, regardless of high uptake into the cells being shown (Figs. 3 and 5). Although L-D35 increases in size with time after the replacement with PBS, H-D35 no longer binds to TLR9. Therefore, rapid uptake into the cells can be required for immune stimulation when using D35 prepared in 50 mM and 100 mM NaCl. Considering these results, L-D35, especially the duplex that is the main component of L-D35, is considered to be suitable for the induction of potent Th-1 immune responses. L-D35 showed not only high cellular uptake but also binding to mTLR9Fc, resulting in induction of the production of a large amount of IFN-α.

In conclusion, we annealed D35 in different NaCl concentrations and evaluated the obtained structures. In water, D35 adopted a single-stranded structure. Meanwhile, in NaCl solution, D35 ODNs adopted a duplex form via palindromic sequences, followed by the formation of quadruplexes in a NaCl concentration-dependent manner. The quadruplexes were formed by parallel and anti-parallel structures. The single-stranded D35 showed poor cellular uptake and no ability to bind to mTLR9Fc proteins. L-D35 showed not only high cellular uptake but also a high affinity to mTLR9Fc proteins, leading to the production of a large amount of IFN-α for PBMCs. Although H-D35 showed high cellular uptake, the affinity to mTLR9Fc proteins decreased, resulting in cytokines for PBMCs not always being induced. These findings suggest that much larger aggregates have difficulty inducing the formation of TLR9 dimers. L-D35 containing the duplex of D35 as the main component is the best structure to induce Th-1 immune responses. Therefore, the findings in this study for D35 ODNs could be a vital research foundation for *in vivo* applications.

Author contributions

Miyu Matsuda: Investigation, Methodology, Writing – original draft. **Shinichi Mochizuki:** Conceptualization, Supervision, Validation, Writing – original draft, Writing – review & editing, Visualization, Funding acquisition.

Funding

This work was supported by JSPS KAKENHI Grant-in-Aid for Scientific Research (B) (JP21H03825), Grant-in-Aid for Challenging Pioneering Research (JP21K19925), Grant-in-Aid for Transformative Research Areas (A) (JP20H05873) in Japan and TaNeDS funding program of Daiichi Sankyo.

Declaration of competing interest

The authors declare that they have no known competing financial interests or personal relationships that could have appeared to influence the work reported in this paper.

Acknowledgments

We would like to gratefully thank Koji Morita and Makoto Koizumi in Daiichi Sankyo Co., Ltd. for their technical advice.

Appendix A. Supplementary data

Supplementary data to this article can be found online at https://doi.org/10.1016/j.bbrep.2023.101573.

References

[1] J. Scheiermann, D.M. Klinman, Clinical evaluation of CpG oligonucleotides as adjuvants for vaccines targeting infectious diseases and cancer, Vaccine 32 (2014) 6377–6389, https://doi.org/10.1016/j.vaccine.2014.06.065.

[2] T. Jakob, P.S. Walker, A.M. Krieg, M.C. Udey, J.C. Vogel, Activation of cutaneous dendritic cells by CpG-containing oligodeoxynucleotides: a role for dendritic cells in the augmentation of Th1 responses by immunostimulatory DNA, J. Immunol. 161 (1998) 3042–3049.

[3] O. Schulz, A.D. Edwards, M. Schito, J. Aliberti, S. Manickasingham, A. Sher, C. Reis e Sousa, CD40 triggering of heterodimeric IL-12 p70 production by dendritic cells in vivo requires a microbial priming signal, Immunity 13 (2000) 453–462, https://doi.org/10.1016/s1074-7613(00)00045-5.

[4] M. Gursel, D. Verthelyi, I. Gursel, K.J. Ishii, D.M. Klinman, Differential and competitive activation of human immune cells by distinct classes of CpG oligodeoxynucleotide, J. Leukoc. Biol. 71 (2002) 813–820.

[5] N. Hanagata, Structure-dependent immunostimulatory effect of CpG oligodeoxynucleotides and their delivery system, Int. J. Nanomed. 7 (2012) 2181–2195, https://doi.org/10.2147/IJN.S30197.

[6] A.M. Krieg, CpG motifs in bacterial DNA and their immune effects, Annu. Rev. Immunol. 20 (2002) 709–760, https://doi.org/10.1146/annurev.immunol.20.100301.064842.

[7] M. Kerkmann, L.T. Costa, C. Richter, S. Rothenfusser, J. Battiany, V. Hornung, J. Johnson, S. Englert, T. Ketterer, W. Heckl, S. Thalhammer, S. Endres, G. Hartmann, Spontaneous formation of nucleic acid-based nanoparticles is responsible for high interferon-alpha induction by CpG-A in plasmacytoid dendritic cells, J. Biol. Chem. 280 (2005) 8086–8093, https://doi.org/10.1074/jbc.M410868200.

[8] C.Y. Lai, G.Y. Yu, Y. Luo, R. Xiang, T.H. Chuang, Immunostimulatory activities of CpG-oligodeoxynucleotides in teleosts: toll-like receptors 9 and 21, Front. Immunol. 10 (2019) 179, https://doi.org/10.3389/fimmu.2019.00179.

[9] D. Verthelyi, K.J. Ishii, M. Gursel, F. Takeshita, D.M. Klinman, Human peripheral blood cells differentially recognize and respond to two distinct CPG motifs, J. Immunol. 166 (2001) 2372–2377, https://doi.org/10.4049/jimmunol.166.4.2372.

[10] M. Kerkmann, S. Rothenfusser, V. Hornung, A. Towarowski, M. Wagner, A. Sarris, T. Giese, S. Endres, G. Hartmann, Activation with CpG-A and CpG-B oligonucleotides reveals two distinct regulatory pathways of type I IFN synthesis in human plasmacytoid dendritic cells, J. Immunol. 170 (2003) 4465–4474, https://doi.org/10.4049/jimmunol.170.9.4465.

[11] F. Steinhagen, C. Meyer, D. Tross, M. Gursel, T. Maeda, S. Klaschik, D.M. Klinman, Activation of type I interferon-dependent genes characterizes the "core response" induced by CpG DNA, J. Leukoc. Biol. 92 (2012) 775–785, https://doi.org/10.1189/jlb.1011522.

[12] J. Vollmer, R. Weeratna, P. Payette, M. Jurk, C. Schetter, M. Laucht, T. Wader, S. Tluk, M. Liu, H.L. Davis, A.M. Krieg, Characterization of three CpG oligodeoxynucleotide classes with distinct immunostimulatory activities, Eur. J. Immunol. 34 (2004) 251–262, https://doi.org/10.1002/eji.200324032.

[13] C. Yu, M. An, M. Li, H. Liu, Immunostimulatory properties of lipid modified CpG oligonucleotide, Mol. Pharm. 14 (2017) 2815–2823, https://doi.org/10.1021/acs.molpharmaceut.7b00335.

[14] H. Liu, K.D. Moynihan, Y. Zheng, G.L. Szeto, A.V. Li, B. Huang, D.S.V. Egeren, C. Park, D.J. Irvine, Structure-based programming of lymph node targeting in molecular vaccines, Nature 507 (2014) 519–522, https://doi.org/10.1038/nature12978.

[15] L.T. Costa, M. Kerkmann, G. Hartmann, S. Endres, P.M. Bisch, W.M. Heckl, S. Thalhammer, Structural studies of oligonucleotides containing G-quadruplex motifs using AFM, Biochem. Biophys. Res. Commun. 313 (2004) 1065–1072, https://doi.org/10.1016/j.bbrc.2003.12.041.

[16] C.C. Wu, J. Lee, E. Raz, M. Corr, D.A. Carson, Necessity of oligonucleotide aggregation for toll-like receptor 9 activation, J. Biol. Chem. 279 (2004) 33071–33078, https://doi.org/10.1074/jbc.M311662200.

[17] T. Aoshi, Y. Haseda, K. Kobiyama, H. Narita, H. Sato, H. Nankai, S. Mochizuki, K. Sakurai, Y. Katakai, Y. Yasutomi, E. Kuroda, C. Coban, K.J. Ishii, Development of nonaggregating poly-A tailed immunostimulatory A/D type CpG oligodeoxynucleotides applicable for clinical use, J. Immunol. Res. 2015 (2015), 316364, https://doi.org/10.1155/2015/316364.

[18] E. Largy, J.L. Mergny, V. Gabelica, Role of alkali metal ions in G-quadruplex nucleic acid structure and stability, Met. Ions Life Sci. 16 (2016) 203–258, https://doi.org/10.1007/978-3-319-21756-7_7.

[19] T. Santos, G.F. Salgado, E.J. Cabrita, C. Cruz, G-Quadruplexes, Their Ligands, Biophysical methods to unravel G-quadruplex/ligand interactions, Pharmaceuticals 14 (2021), https://doi.org/10.3390/ph14080769.

[20] L. Haase, K. Weisz, Locked nucleic acid building blocks as versatile tools for advanced G-quadruplex design, Nucleic Acids Res. 48 (2020) 10555–10566, https://doi.org/10.1093/nar/gkaa720.

[21] P.M. Toro, M. Saldias, G. Valenzuela-Barra, Metal-organic compounds as anticancer agents: versatile building blocks for selective action on G-quadruplexes, Curr. Med. Chem. 30 (2023) 573–600, https://doi.org/10.2174/0929867329666220606160209.

[22] A.T.T. Tu, K. Hoshi, K. Ikebukuro, N. Hanagata, T. Yamazaki, Monomeric G-quadruplex-based CpG oligodeoxynucleotides as potent toll-like receptor 9 agonists, Biomacromolecules 21 (2020) 3644–3657, https://doi.org/10.1021/acs.biomac.0c00679.

[23] J. Kypr, I. Kejnovska, D. Renciuk, M. Vorlickova, Circular dichroism and conformational polymorphism of DNA, Nucleic Acids Res. 37 (2009) 1713–1725, https://doi.org/10.1093/nar/gkp026.

[24] M. Vorlickova, J. Sagi, Transitions of poly(dI-dC), poly(dI-methyl5dC) and poly(dI-bromo5dC) among and within the B-, Z-, A- and X-DNA families of conformations, Nucleic Acids Res. 19 (1991) 2343–2347, https://doi.org/10.1093/nar/19.9.2343.

[25] S. Paramasivan, I. Rujan, P.H. Bolton, Circular dichroism of quadruplex DNAs: applications to structure, cation effects and ligand binding, Methods 43 (2007) 324–331, https://doi.org/10.1016/j.ymeth.2007.02.009.
[26] D.M. Gray, J.D. Wen, C.W. Gray, R. Repges, C. Repges, G. Raabe, J. Fleischhauer, Measured and calculated CD spectra of G-quartets stacked with the same or opposite polarities, Chirality 20 (2008) 431–440, https://doi.org/10.1002/chir.20455.
[27] R. Yu, B. Zhu, D. Chen, Type I interferon-mediated tumor immunity and its role in immunotherapy, Cell, Mol. Life Sci. 79 (2022) 191, https://doi.org/10.1007/s00018-022-04219-z.
[28] G. Laughlan, A.I. Murchie, D.G. Norman, M.H. Moore, P.C. Moody, D.M. Lilley, B. Luisi, The high-resolution crystal structure of a parallel-stranded guanine tetraplex, Science 265 (1994) 520–524, https://doi.org/10.1126/science.8036494.
[29] B.H. Ruan, X. Li, A.R. Winkler, K.M. Cunningham, J. Kuai, R.M. Greco, K.H. Nocka, L.J. Fitz, J.F. Wright, D.D. Pittman, X.Y. Tan, J.E. Paulsen, L.L. Lin, D.G. Winkler, Complement C3a, CpG oligos, and DNA/C3a complex stimulate IFN-alpha production in a receptor for advanced glycation end product-dependent manner, J. Immunol. 185 (2010) 4213–4222, https://doi.org/10.4049/jimmunol.1000863.
[30] A.P. Moseman, E.A. Moseman, S. Schworer, I. Smirnova, T. Volkova, U. von Andrian, A. Poltorak, Mannose receptor 1 mediates cellular uptake and endosomal delivery of CpG-motif containing oligodeoxynucleotides, J. Immunol. 191 (2013) 5615–5624, https://doi.org/10.4049/jimmunol.1301438.
[31] Y. Kimura, K. Sonehara, E. Kuramoto, T. Makino, S. Yamamoto, T. Yamamoto, T. Kataoka, T. Tokunaga, Binding of oligoguanylate to scavenger receptors is required for oligonucleotides to augment NK cell activity and induce IFN, J. Biochem. 116 (1994) 991–994, https://doi.org/10.1093/oxfordjournals.jbchem.a124658.
[32] H. Irie, K. Morita, M. Koizumi, S. Mochizuki, Immune responses and antitumor effect through delivering to antigen presenting cells by optimized conjugates consisting of CpG-DNA and antigenic peptide, bioconjug, Chem 31 (2020) 2585–2595, https://doi.org/10.1021/acs.bioconjchem.0c00523.
[33] E. Latz, A. Verma, A. Visintin, M. Gong, C.M. Sirois, D.C. Klein, B.G. Monks, C. J. McKnight, M.S. Lamphier, W.P. Duprex, T. Espevik, D.T. Golenbock, Ligand-induced conformational changes allosterically activate Toll-like receptor 9, Nat. Immunol. 8 (2007) 772–779, https://doi.org/10.1038/ni1479.
[34] J. Chen, S. Nag, P.A. Vidi, J. Irudayaraj, Single molecule in vivo analysis of toll-like receptor 9 and CpG DNA interaction, PLoS One 6 (2011), e17991, https://doi.org/10.1371/journal.pone.0017991.